Journal of Applied Polymer Science

Preparation and properties of novel, flexible, lead-free X-ray-shielding materials containing tungsten and bismuth(III) oxide

Hao Chai,[1] Xiaobin Tang,[1,2] Minxuan Ni,[1] Feida Chen,[1] Yun Zhang,[1] Da Chen,[1,2] Yunlong Qiu[3]
[1]Department of Nuclear Science and Engineering, Nanjing University of Aeronautics and Astronautics, Nanjing 211100, China
[2]Jiangsu Key Laboratory of Nuclear Energy Equipment Materials Engineering, Nanjing 211100, China
[3]ZhongXing Energy Equipment Company, Limited, Haimen Nantong 226100, China
Correspondence to: X. Tang (E-mail: tangxiaobin@nuaa.edu.cn)

ABSTRACT: Novel, flexible, lead-free X-ray-shielding composites were prepared with a high-functional methyl vinyl silicone rubber (VMQ) matrix with W and Bi_2O_3 as filler materials. To verify the advanced properties of the lead-free material, composites with the same mass fraction of PbO were compared. With the X-ray energy ranging from 48 to 185 keV, the W/Bi_2O_3/VMQ composites exhibited higher X-ray-shielding properties. As the filler volume fraction decreased, the tensile strength, elongation, tear strength, and flexibility of the W/Bi_2O_3/VMQ composites increased. The Shore hardness of the W/Bi_2O_3/VMQ composites had a maximum value of 46.6 HA and was still very flexible. With decreasing filler volume fraction, the water-vapor transmission performances of the W/Bi_2O_3/VMQ composites increased, and the W/Bi_2O_3/VMQ composites also showed better water-vapor permeability. The heat-transfer properties of the W/Bi_2O_3/VMQ composites increased with increasing W content, and when the W content exceeded 70 wt %, the thermal conductivity of the W/Bi_2O_3/VMQ material was about 70.45% higher than that of the PbO/VMQ composite. © 2015 Wiley Periodicals, Inc. J. Appl. Polym. Sci. **2016**, *133*, 43012.

KEYWORDS: composites; mechanical properties; properties and characterization; thermal properties

Received 13 July 2015; accepted 29 September 2015
DOI: 10.1002/app.43012

INTRODUCTION

With the rapid development of science and technology, nuclear technology has been widely used in X-ray diagnostic departments,[1–3] but the associated hazards have prompted increasing concerns for individual radiation protection and safety. Many studies have been carried out on medical radiation shielding because shielding is directly related to the prevention of radiation poisoning in patients and health professionals.[4–6] Lead rubber has γ-/X-ray-shielding properties and a certain flexibility, so some radiation-shielding clothing and radiation-shielding curtains are made of lead rubber.[7] On the other hand, the toxicity of lead as a heavy metal is a major concern, and there are a range of studies related to this in terms of occupational exposure and *in vivo* absorption.[8–10] Moreover, the flexibility and aging resistance of rubbers are somewhat inadequate. On the basis of this, the research and development of lead-free radiation-shielding materials have been reported, such as that into lead-free radiation-shielding glass[11,12] and lead-free polymer composites.[13–17] Nevertheless, the research into flexible, lead-free, γ/X-ray-shielding materials is rare. Hence, the study of flexible lead-free material was deemed significant for individual γ/X-ray protective clothing items.

Compared with high energy rays, the absorption of low energy rays was more obviously affected by the edge absorption of radiation-shielding elements. The radiation-shielding abilities of materials could be affected by the types, and proportions, of functional elements present. In this research, a new flexible lead-free X-ray radiation-shielding material was fabricated by silicone rubber mixing and vulcanized molding. Vinyl silicone rubber (VMQ) material was used as the matrix; platinum vulcanizing agents (group A and group B) were also used, along with W and Bi_2O_3 as functional powder fillers. A flexible, PbO powder-loaded X-ray radiation-shielding material was also prepared by this method. The authors have presented a comparison of X-ray-shielding properties in terms of transmission factor parameters, mechanical properties, water-vapor transmission performance, and thermal conductivity of W/Bi_2O_3/VMQ, W/VMQ, Bi_2O_3/VMQ and PbO/VMQ composites.

EXPERIMENTAL

Materials

The following were used to prepare flexible X-ray-shielding materials: W powder (>99%, ~6 μm, Zhuzhou Cemented Carbide Group Co. Limited, China), Bi_2O_3 powder (>99%, ~2 μm, Hunan Jin Tai Bismuth Industry Co. Limited, China), PbO

Table I. Compositions of Different Samples

Sample	VMQ matrices (wt %)	W powder (wt %)	Bi_2O_3 powder (wt %)	PbO powder (wt %)
1	20	10	70	
2	20	20	60	
3	20	30	50	
4	20	40	40	
5	20	50	30	
6	20	60	20	
7	20	70	10	
8	20	80		
9	20		80	
10	20			80

powder (>99%, ~10 μm, Sinopharm Reagent, China), VMQ (110-3, > 95%, Dongjue Silicone Group Co. Limited, China), platinum vulcanizing agent group A (3000 ppm, Shanghai Farida Chemical Co. Limited, China), and platinum vulcanizing agent group B (4000 ppm, Shanghai Farida Chemical Co. Limited, China).

Preparation of Composites

Samples of W/Bi_2O_3/VMQ, W/VMQ, Bi_2O_3/VMQ and PbO/VMQ composites were prepared by silicone rubber mixing and vulcanized molding processes. The VMQ matrices, and uncured VMQ composites, were all fabricated in a mixing mill. The VMQ matrices were prepared by two-step mechanical mixing. First, the VMQ and platinum vulcanizing agent (group B) were mill-mixed for 10 min with a mixing weight ratio of 100:2. Then, the mixture and platinum vulcanizing agent (group A) were mixed for 10 min with a mixing weight ratio of 100:1. The uncured VMQ composites were also prepared by the mechanical

Figure 1. Flexible X-ray-shielding VMQ composite samples. [Color figure can be viewed in the online issue, which is available at wileyonlinelibrary.com.]

mixing of VMQ matrices and filler powders for 15 min. The filler properties are summarized in Table I.

The VMQ composite samples were fabricated by vulcanized molding in a plate-vulcanizing machine. The uncured VMQ composites were placed into a mold coated with a release agent. The mold was loaded to an applied pressure of 10 MPa with a plate-vulcanizing machine after the release cloths were covered. The VMQ composites were cured in the mold for 15 min at 175°C. Finally, the VMQ composite samples were postcured in a fan-assisted drying cabinet for 4 h at 200°C. The flexible VMQ composite samples featured a plate-type structure with dimensions of 100 × 100 × 2 mm^3 (Figure 1); samples 1–7 were W/Bi_2O_3/VMQ composites, sample 8 was a W/VMQ composite, sample 9 was a Bi_2O_3/VMQ composite, and sample 10 was a PbO/VMQ composite.

X-ray-shielding Measurements

The mass attenuation coefficient (μ/ρ) of these functional fillers was obtained with WinXCOM computer software. This software was developed by the National Institute of Standards and Technology.[18] Experimental measurements were performed to investigate the X-ray attenuation in these composites. X-rays were generated by a standard X-ray machine (MG-325, Germany), and an NaI detector was used to test the X-ray changes before and after they passed through the samples. The shielding performances of the W/Bi_2O_3/VMQ, W/VMQ, Bi_2O_3/VMQ, and PbO/VMQ composites were tested at tube voltages of 55, 70, 100, 125, 170, and 210 kV, respectively. The average X-ray energies were 48, 60, 87, 109, 149, and 185 keV, respectively. The transmission factor was used to estimate the X-ray-shielding properties of the composites. A schematic of the apparatus is show in Figure 2.

Morphology Observations

The fracture surface morphologies of the W/Bi_2O_3/VMQ, W/VMQ, Bi_2O_3/VMQ, and PbO/VMQ composites were observed by scanning electron microscopy (SEM; JSM-7500, JEOL). The fracture surfaces of the VMQ composites after tensile testing were investigated to assess the interfacial adhesion and dispersion quality of the filler particles.

Mechanical Properties

The mechanical properties of the W/Bi_2O_3/VMQ, W/VMQ, Bi_2O_3/VMQ, and PbO/VMQ composites were evaluated at

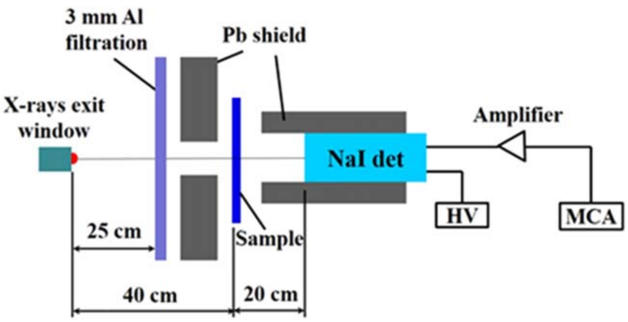

Figure 2. Schematic of the apparatus used to measure the X-ray-shielding performance of the VMQ composites. HV = high voltage; MCA = multichannel analyzer. [Color figure can be viewed in the online issue, which is available at wileyonlinelibrary.com.]

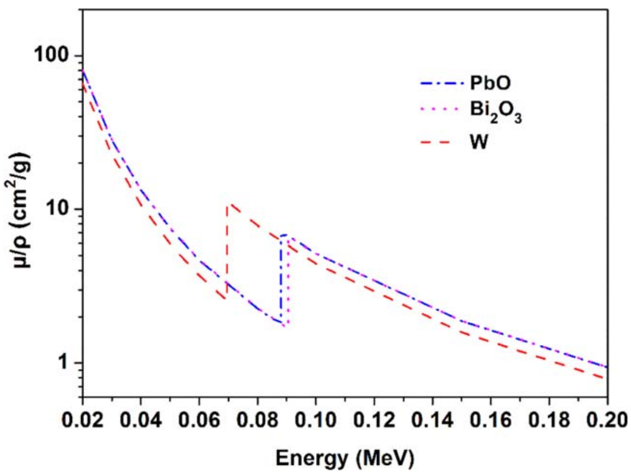

Figure 3. Photon-radiation-shielding abilities of the functional particles. [Color figure can be viewed in the online issue, which is available at wileyonlinelibrary.com.]

room temperature with a mechanical testing machine (WANCE ETM-D). Tensile tests (ASTM D 412) were conducted at a displacement rate of 500 mm/min, and tearing tests (ASTM D 624) were conducted at 50 mm/min. Shore hardness tests were performed with a Shore A durometer according to the ASTM D 2240 standard.

Water-Vapor Transmission Measurements

The water-vapor transmission performances of the W/Bi_2O_3/VMQ, W/VMQ, Bi_2O_3/VMQ, and PbO/VMQ composites were tested by the water method (ASTM E 96). The test dishes were filled with distilled water, covered with 2 mm thick VMQ composite samples, and sealed with asphalt. The test dishes were placed in a fan-assisted drying cabinet for 6 h at 40°C; then, the changes in the mass of each test dish were measured on a high-sensitivity balance. The average cumulative permeation was used to estimate the water-vapor transmission performance of the VMQ materials.

Thermal Conductivity Measurements

The thermal conductivity of the W/Bi_2O_3/VMQ, W/VMQ, Bi_2O_3/VMQ, and PbO/VMQ composites was tested with a thermal conductivity instrument (XIANGKE DRL-3) according to ASTM D 5470. The thermal conductivity was used to estimate the heat-transfer properties of the VMQ composites.

RESULTS AND DISCUSSION

X-ray-Shielding Properties

To find the differences in radiation-shielding ability among the functional particles, the μ/ρ values of W, Bi_2O_3, and PbO were simulated with WinXCOM, and the results are shown in Figure 3. When the energy of γ/X-rays was lower, W, Bi_2O_3, and PbO had different radiation-shielding abilities; these were related to the edge absorption of the elements. So, the stronger and weaker absorption regions of each functional particle are shown in Figure 3. W, Bi_2O_3, and PbO showed boundary energies at the threshold between the stronger and weaker absorption of approximately 0.0695, 0.0905, and 0.088 MeV, respectively. Furthermore, the stronger absorption region of W and the weaker absorption regions of Bi_2O_3 and PbO were complementary. Hence, W and Bi_2O_3, with that coordination ratio, could remedy the weaker absorption region of Bi_2O_3, and the radiation-shielding ability of W/Bi_2O_3/VMQ material may be better than Bi_2O_3/VMQ and PbO/VMQ materials at some X-ray energies.

The X-ray-shielding characteristics of the W/Bi_2O_3/VMQ, W/VMQ, Bi_2O_3/VMQ, and PbO/VMQ composites at 80 wt % filler particles were determined. The X-ray transmission factor (I/I_0) was used to assess the photon-shielding properties, where I and I_0 are the intensity of the incident X-ray beam and that transmitted through the thickness direction of the sample composites, respectively. Figure 4 shows the X-ray flux attenuation properties of the 2 mm thick VMQ composites. The PbO/VMQ and Bi_2O_3/VMQ materials revealed I/I_0 values of 0.39 and 0.35, respectively, at a 100-kV X-ray-tube voltage. With increasing W content, the transmission factors of the W/Bi_2O_3/VMQ materials decreased at this 100-kV X-ray-tube voltage. This was because the average X-ray energy at a 100-kV tube voltage was 87 keV. The weaker absorption region of PbO and Bi_2O_3 occurred at an X-ray energy of 87 keV, so the PbO/VMQ and Bi_2O_3/VMQ composites exhibited weaker X-ray-shielding performances at this energy. The stronger absorption region of W and the weaker absorption region of Bi_2O_3 also occurred at an X-ray energy of 87 keV; hence, Bi_2O_3, mixed with W, could remedy the weaker absorption region of Bi_2O_3. That is why the W/VMQ and W/Bi_2O_3/VMQ materials exhibited better X-ray-shielding abilities than the PbO/VMQ and Bi_2O_3/VMQ composites. In Figure 4, the X-ray-shielding properties of samples 5, 6, and 7 corresponded to the W/VMQ composite. However, the price of W is much higher than that of Bi_2O_3, so the W/Bi_2O_3/VMQ composites are more valuable than W/VMQ for use.

Morphological Observations

The fracture surfaces of the W/Bi_2O_3/VMQ, W/VMQ, Bi_2O_3/VMQ, and PbO/VMQ composites, after tensile testing, were investigated to determine the interfacial adhesion and dispersion quality of the filler particles. Figure 5(a–j) shows the SEM micrographs of the fracture surfaces of samples 1–10,

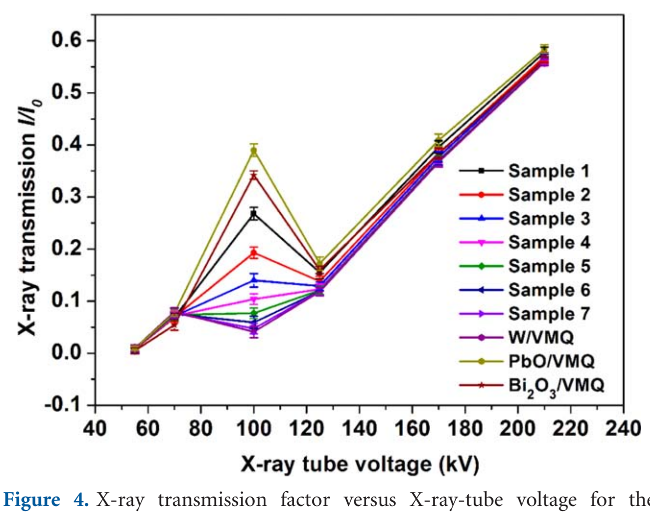

Figure 4. X-ray transmission factor versus X-ray-tube voltage for the VMQ samples. [Color figure can be viewed in the online issue, which is available at wileyonlinelibrary.com.]

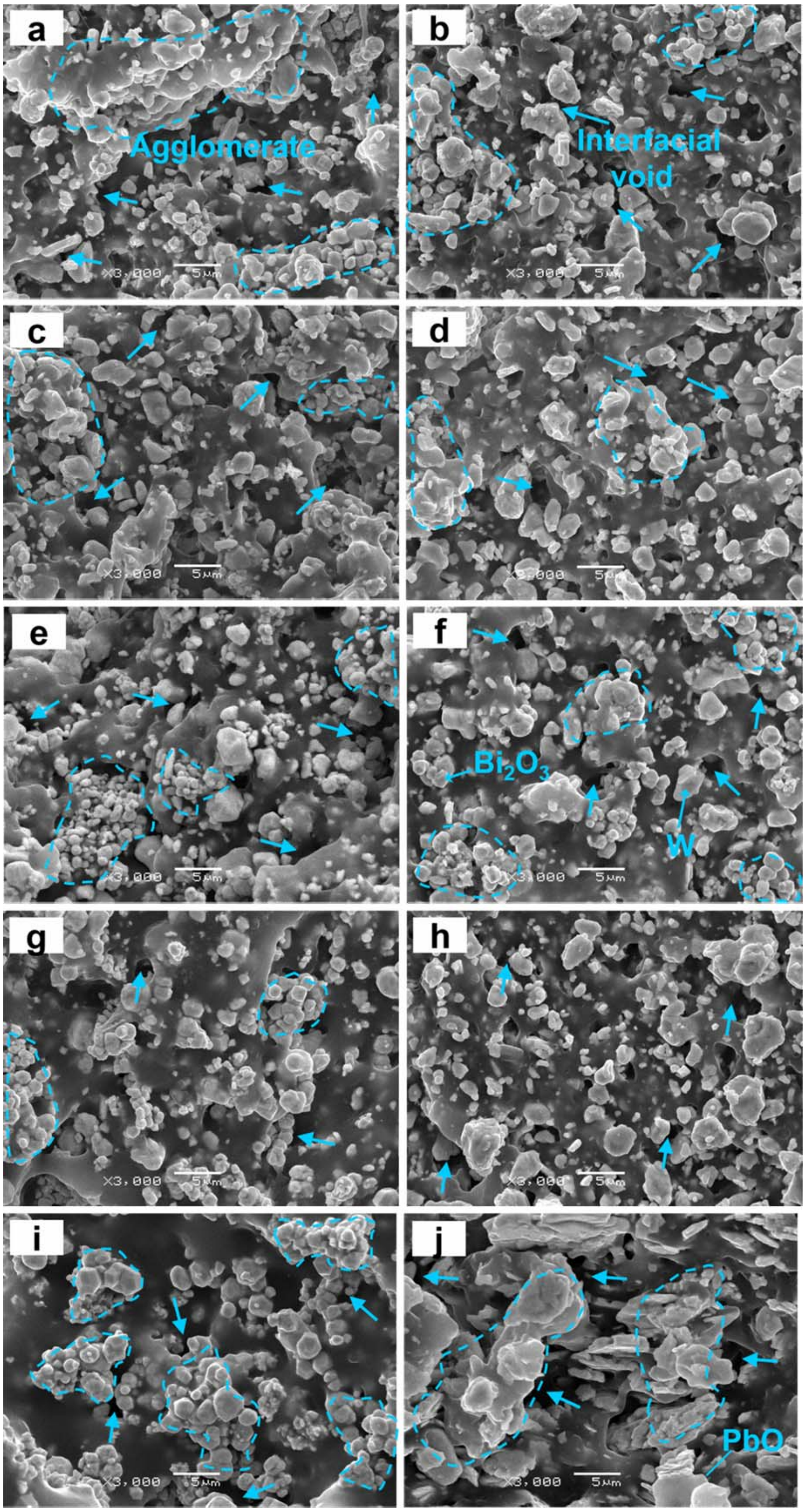

Figure 5. SEM micrographs of the fractured surfaces of the VMQ composites: samples (a) 1, (b) 2, (c) 3, (d) 4, (e) 5, (f) 6, (g) 7, (h) 8, (i) 9, and (j) 10. [Color figure can be viewed in the online issue, which is available at wileyonlinelibrary.com.]

Table II. Mechanical Properties of the VMQ Composites

Sample	Filler volume fraction (%)	Tensile strength (MPa)	Elongation at break (%)	Tear strength (KN/m)	Shore hardness (HA)
1	30.86	1.06 ± 0.03	150.6 ± 24	0.69 ± 0.10	46.6 ± 0.9
2	29.28	1.14 ± 0.02	384.3 ± 29	0.69 ± 0.12	40.7 ± 0.8
3	27.63	1.24 ± 0.03	466.4 ± 35	0.75 ± 0.13	37.8 ± 0.7
4	25.75	1.35 ± 0.04	539.9 ± 28	0.88 ± 0.11	34.3 ± 0.4
5	24.08	1.39 ± 0.03	677.6 ± 42	1.45 ± 0.15	32.7 ± 0.5
6	22.17	1.51 ± 0.04	891.5 ± 33	4.60 ± 0.18	28.0 ± 0.4
7	20.16	1.66 ± 0.03	1132.7 ± 47	5.45 ± 0.16	25.3 ± 0.7
8	18.04	1.71 ± 0.02	1250.2 ± 35	5.83 ± 0.12	19.4 ± 0.8
9	32.37	1.01 ± 0.04	110.3 ± 22	0.65 ± 0.11	52.5 ± 0.6
10	30.89	1.05 ± 0.02	115.1 ± 17	0.73 ± 0.13	53.7 ± 0.9

respectively. Agglomerates and interfacial voids are marked in the SEM micrographs. According to their different particle sizes and shapes, the polygonal particles, white near-spherical particles, and flaky grains indicate W, Bi_2O_3, and PbO, respectively. The filler contents of the W/Bi_2O_3/VMQ, W/VMQ, Bi_2O_3/VMQ, and PbO/VMQ composites are summarized in Table I. As shown in Figure 5(a–h), the number of filler particles gradually decreased, and the size and number of agglomerates gradually decreased. Moreover, many Bi_2O_3 and PbO agglomerates are also shown in Figure 5(i,j). This finding indicated that the number of agglomerates of these composites increased with increasing filler volume fraction. From the SEM images, the VMQ composites with high filler volume fractions apparently had more defects.

Mechanical Properties

The mechanical properties of radiation-shielding materials are important in determining material service conditions. The mechanical properties of the VMQ-based photon-shielding materials with different filler compositions at room temperature are shown in Table II. Because of the higher density of W (19.35 g/cm^3) compared to those of Bi_2O_3 (8.9 g/cm^3) and PbO (9.53 g/cm^3), the filler volume fraction of the W/Bi_2O_3/VMQ composites decreased with increasing W content, and the W/VMQ material had the lowest filler volume fraction. The tensile properties of the composites were characterized by tensile strength and elongation at break testing. The W/Bi_2O_3/VMQ and W/VMQ composites exhibited better tensile performances than the Bi_2O_3/VMQ and PbO/VMQ composites, and as the filler volume fraction decreased, the tensile strengths and elongations of the W/Bi_2O_3/VMQ composites increased. This may have been due to more defects in the matrix appearing when the filler volume fraction increased, and the tensile strength and elongation of the composites were weakened by the presence of defects. The W/Bi_2O_3/VMQ and W/VMQ composites also exhibited better tear strengths than the Bi_2O_3/VMQ and PbO/VMQ composite: as the filler volume fraction decreased, the tear strengths of the W/Bi_2O_3/VMQ composites increased. This phenomenon was attributed to the high levels of filler volume fraction caused by agglomeration and interfacial voids around the particles in the matrix; this impaired the continuity of the structure and formed stress concentrations within the composites. This resulted in their weaker tear strength.[19] The filler content and hardness were important factors influencing the Shore hardness of these composites. The W/Bi_2O_3/VMQ and W/VMQ composites displayed a lower Shore hardness than the Bi_2O_3/VMQ and PbO/VMQ materials. In this study, the VMQ material had a low Shore hardness, but the filler particles had a high Shore hardness. Thus, the Shore hardness of the VMQ-based composites increased with increasing filler volume fraction, and the maximum Shore hardness of the W/Bi_2O_3/VMQ material was 46.6 ± 0.9 HA, but the sample also retained its flexibility. The W/VMQ composite had the best mechanical properties, but the price of the price of W was much higher than that of Bi_2O_3. So, the W/Bi_2O_3/VMQ composites could obviously reduce the cost of the materials without compromising security.

Water-Vapor Transmission Performances

Perspiration from the wearer is more easily permeated when radiation-shielding garment materials exhibit a certain water-vapor transmission performance. Hence, the comfort of workers is increased, especially if they are required to wear radiation-shielding garments for longer periods of time. In this study, the water-vapor transmission performances of the W/Bi_2O_3/VMQ, W/VMQ, Bi_2O_3/VMQ, and PbO/VMQ composites were investigated, and the results are shown in Table III. The average cumulative permeations for the Bi_2O_3/VMQ and PbO/VMQ composite were 0.441 ± 0.004 and 0.442 ± 0.003 g h^{-1} m^{-2}; these values were less than those of the W/Bi_2O_3/VMQ and W/VMQ materials. With decreasing filler volume fraction, the average cumulative permeability of the W/Bi_2O_3/VMQ composites increased. The experimental results show that the filler volume fractions had an important influence on the water-vapor transmission performance of these composites. This may have been because, with the filler volume fraction increasing, the number of effective barrier units in the VMQ composites also increased. So, the gas barrier properties of the VMQ composites increased with increasing filler volume fraction.[20,21]

Thermal Conductivity

Because flexible radiation-shielding clothing materials should exhibit excellent heat-transfer performance and increase human

Table III. Water-Vapor Transmission Performances of the VMQ Composites

Sample	Filler volume fraction (%)	Average cumulative permeation (g h^{-1} m^{-2})
1	30.86	0.445 ± 0.003
2	29.28	0.451 ± 0.004
3	27.63	0.458 ± 0.005
4	25.75	0.470 ± 0.002
5	24.08	0.483 ± 0.004
6	22.17	0.502 ± 0.003
7	20.16	0.526 ± 0.005
8	18.04	0.539 ± 0.003
9	32.37	0.441 ± 0.004
10	30.89	0.442 ± 0.003

comfort, the thermal conductivities of these materials also had to be evaluated. Figure 6 shows the thermal conductivities of the W/Bi_2O_3/VMQ, W/VMQ, Bi_2O_3/VMQ, and PbO/VMQ composites. The thermal conductivity of polymeric composites is mainly governed by the types and contents of their particulate fillers. The thermal conductivity of the neat VMQ, Bi_2O_3/VMQ, and PbO/VMQ materials were 0.27, 0.428, and 0.4184 W m^{-1} K^{-1}, respectively. The thermal conductivities of the W/Bi_2O_3/VMQ composites increased with increasing W content. The W/Bi_2O_3/VMQ and W/VMQ composites showed higher effective thermal conductivities than the Bi_2O_3/VMQ and PbO/VMQ composites at the same filler mass fraction. This phenomenon could have been due to the higher thermal conductivities of W (174 W m^{-1} K^{-1}) and Bi_2O_3 (3.53 W m^{-1} K^{-1}) compared to PbO (3.16 W m^{-1} K^{-1}). When the W content exceeded 70 wt %, the thermal conductivity of the W/Bi_2O_3/VMQ material was 70.45% higher than that of the PbO/VMQ composite. In this study, we was confirmed that W efficiently increased the thermal conductivity of the VMQ composites and thus provided potential applications in the preparation of better heat-transfer photon-radiation-shielding materials.

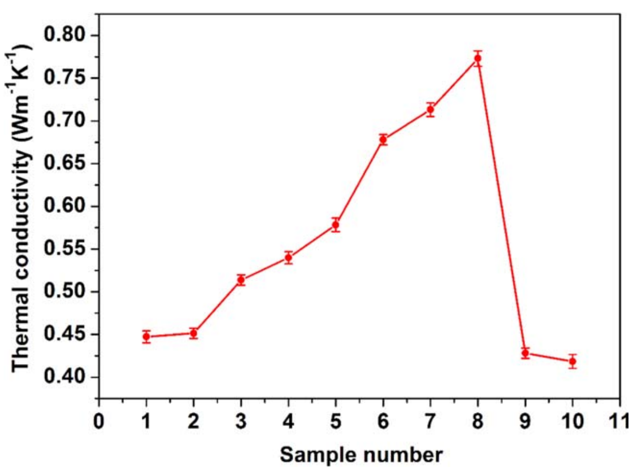

Figure 6. Effective thermal conductivity of W/Bi_2O_3/VMQ, W/VMQ, Bi_2O_3/VMQ, and PbO/VMQ composites. [Color figure can be viewed in the online issue, which is available at wileyonlinelibrary.com.]

CONCLUSIONS

W/Bi_2O_3/VMQ γ-/X-ray-shielding composites were fabricated by silicone rubber mixing and vulcanized molding. To verify the advanced performances of the lead-free material, W/VMQ, Bi_2O_3/VMQ, and PbO/VMQ composites with the same filler mass fractions were compared. The X-ray-shielding properties, mechanical properties, water-vapor transmission performances, and thermal conductivities of the W/Bi_2O_3/VMQ, W/VMQ, Bi_2O_3/VMQ, and PbO/VMQ composites were compared. The W/Bi_2O_3/VMQ and W/VMQ composites exhibited better X-ray-shielding properties than the Bi_2O_3/VMQ and PbO/VMQ composites, especially at an X-ray energy of 87 keV. The W/Bi_2O_3/VMQ and W/VMQ composites also exhibited better mechanical properties than the Bi_2O_3/VMQ and PbO/VMQ composites, and with decreasing filler volume fraction, the tensile strength, elongation, tear strength, and flexibility of the W/Bi_2O_3/VMQ composites increased. The Shore hardness of the W/Bi_2O_3/VMQ composites had a maximum value of 46.6 HA but remained sufficiently flexible. The water-vapor transmission performance of the W/Bi_2O_3/VMQ composites also increased with decreasing filler volume fraction, and the W/Bi_2O_3/VMQ and W/VMQ composites allowed greater water-vapor transmission than Bi_2O_3/VMQ and PbO/VMQ composites. The thermal conductivity of W/Bi_2O_3/VMQ composite was enhanced with increasing W content. When the W content exceeded 70 wt %, the thermal conductivity of the W/Bi_2O_3/VMQ material was 70.45% higher than that of the PbO/VMQ composite.

The W/VMQ composite had better properties but a high cost. The W/Bi_2O_3/VMQ composites obviously reduced the cost of materials without compromising security. The W/Bi_2O_3/VMQ material developed here featured excellent flexibility, γ-/X-ray-shielding performance, thermal conductivity, and a certain water-vapor transmission and might be a better material for the manufacture of radiation-shielding garments.

ACKNOWLEDGMENTS

This work was supported by the National Defense Basic Scientific Research Project (grant B2520133007), the Cooperative Innovation Fund Project of Jiangsu Province (grant BY2014003-04), the Funding of Jiangsu Innovation Program for Graduate Education (grant SJZZ_0040), and the A Project of the Priority Academic Program Development of Jiangsu Higher Education Institutions.

REFERENCES

1. Lin, Z.; Xu, Q.; Zhang, K. B.; Zhang, Z. G.; Liu, X. S.; Zhao, L. Q.; Lin, C. Y.; Li, Y.; Hua, X. L.; Zhao, H. L.; Hua, J.; Xu, J. R. *Acta Radiol.* **2015**, *56*, 552.
2. Berkowitz, E. A.; Henry, T. S.; Veeraraghavan, S. G.; Staton, W.; Gal, A. A. *Am. J. Roentgenol.* **2015**, *204*, 750.

3. Fukuhara, T.; Fujiwara, K.; Fujii, T.; Takeda, K.; Matsuda, E.; Hasegawa, K.; Nomura, K.; Kitano, H. *Auris Nasus Larynx* **2015**, *42*, 49.
4. Schmid, E.; Panzer, W.; Schlattl, H.; Eder, H. *J. Radiol. Prot.* **2012**, *32*, N129.
5. Kim, S. C.; Dong, K. R.; Chung, W. K. *Ann. Nucl. Energy* **2012**, *47*, 1.
6. Kim, S. C.; Dong, K. R.; Chung, W. K. *J. Korean Phys. Soc.* **2012**, *60*, 165.
7. Gwaily, S. E.; Madani, M.; Hassan, H. H. *Polym. Compos.* **2002**, *23*, 495.
8. Kim, S. C.; Park, M. H. *J. Radiol. Sci. Technol.* **2011**, *34*, 141.
9. Healey, N. *Radiat. Prot. Dosim.* **2009**, *134*, 143.
10. Murata, K.; Lwata, T.; Dakeishi, M.; Karita, K. *J. Occup. Health* **2009**, *51*, 1.
11. Kaewkhao, J.; Pokaipisit, A.; Limsuwan, P. *J. Nucl. Mater.* **2010**, *399*, 38.
12. Bootjomchai, C.; Laopaiboon, J.; Yenchai, C.; Laopaiboon, R. *Radiat. Phys. Chem.* **2012**, *81*, 785.
13. Wang, H. B.; Zhang, H.; Su, Y.; Liu, T.; Yu, H. Y.; Yang, Y. H.; Li, X. D.; Guo, B. *Polym. Compos.* **2015**, *36*, 651.
14. Yue, K.; Luo, W. Y.; Dong, X. Q.; Wang, C. S.; Wu, G. H.; Jiang, M. W.; Zha, Y. Z. *Radiat. Prot. Dosim.* **2009**, *133*, 256.
15. Kim, J.; Seo, D.; Lee, B. C.; Seo, Y. S.; Miller, W. H. *Adv. Eng. Mater.* **2014**, *16*, 1083.
16. Nambiar, S.; Osei, E. K.; Yeow, J. T. W. *J. Appl. Polym. Sci.* **2013**, *127*, 4939.
17. Mao, Y. Y.; Zhi, X.; Hu, S.; Ma, X. J.; Wen, S. P.; Fong, H.; Liu, L. *J. Compos. Mater.* **2015**, *49*, 1989.
18. Shirmardi, S. P.; Shamsaei, M.; Naserpour, M. *Ann. Nucl. Energy* **2013**, *55*, 288.
19. Lee, M. K.; Lee, J. K.; Kim, J. W.; Lee, G. J. *J. Nucl. Mater.* **2014**, *445*, 63.
20. Zhang, Y. D.; Liu, Q. F.; Li, H. P.; Lu, Y. P.; Zhang, Q. *New Chem. Mater.* **2010**, *38*, 103.
21. Wang, Z. F.; Wang, B.; Qi, N.; Zhang, H. F.; Zhang, L. Q. *Polymer* **2005**, *46*, 719.